

Facile Fabrication of an Amentoflavone-Loaded Micelle System for Oral Delivery To Improve Bioavailability and Hypoglycemic Effects in KKAY Mice

Junxia Zhang,^{†,‡,§} Jichun Zhou,[†] Tingting Zhang,[†] Zhenxi Niu,^{‡,||} Juan Wang,[†] Jiaomei Guo,[†] Zhenguo Li,[†] and Zhenzhong Zhang^{*,‡,§}

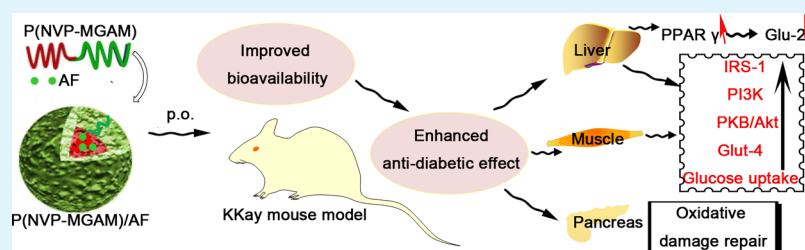
[†]Henan Institute for Food and Drug Control, Zhengzhou 543000, P. R. China

[‡]School of Pharmaceutical Sciences, Zhengzhou University, 100 Kexue Avenue, Zhengzhou 450001, P. R. China

[§]Key Laboratory of Targeting Therapy and Diagnosis for Critical Diseases, Zhengzhou 450001, Henan Province, P. R. China

^{||}College of Pharmacy, Children's Hospital Affiliated to Zhengzhou University, Zhengzhou 450018, P. R. China

Supporting Information



ABSTRACT: In order to increase the oral bioavailability and antidiabetic effect of amentoflavone with multimechanisms, an oral micelle system was developed by using a *N*-vinyl pyrrolidone-maleate-guerbet alcohol monoester polymer for the first time, which was designated as P(NVP-MGAM)/AF. After oral administration, P(NVP-MGAM)/AF enhanced the oral bioavailability of amentoflavone, which was approximately 3.2 times that of amentoflavone solution. The animal study using the KKAY insulin-resistant diabetes mouse model indicated that it regulates the expression and activity of downstream signaling factors and proteins by lowering blood lipids, reducing inflammatory responses and activating the peroxisome proliferator-activated receptor (PPAR) γ signaling pathway and PI3K/Akt signaling pathway. After being made into micelles, it is more effective because of its better absorbability and bioavailability. The results from this study provide a theoretical basis for the clinical application of amentoflavone for diabetes treatment. The oral micelles of P(NVP-MGAM)/AF may become one of the most potent drugs in the treatment of diabetes mellitus, which opens up a new way for the prevention and treatment of diabetes.

KEYWORDS: amentoflavone, oral micelle, *N*-vinyl pyrrolidone-maleate-guerbet alcohol monoester polymer, type 2 diabetes mellitus, bioavailability

1. INTRODUCTION

Diabetes mellitus is one of the most aggressive health concerns for humans.^{1,2} A representative pathological phenomenon of diabetes is associated with the dysfunction of glucose regulation, which involves signs such as nephropathy, retinal diabetic neurodegeneration, and so on, leading to serious morbidity.³ Moreover, the majority of diabetic individuals can be classified as type 2 diabetes mellitus (T2DM), which shows typical characters: hyperglycemia, hyperinsulinism, elevated plasma galanin levels, and decreased galanin receptor activities.⁴ With the development of antidiabetic agents, there has been great interest in botanicals as a source for alternative therapy for chronic diseases, including diabetes.^{5–7} *Selaginella tamariscina* or *Ginkgo biloba* is a kind of herb with a long history of medicinal use.⁸ Recently, the extract of its leaves, amentoflavone, was shown to inhibit α -glucosidase and control of dipeptidyl peptidase IV activity.^{9,10} Despite these

mechanisms reported by these studies, a comprehensive cellular mechanism of action in vivo also requires considerable investigation at multiple tissues, such as coordinated mechanisms from liver, adipocytes, and skeletal muscle. However, the bioavailability of amentoflavone with po administration was $0.04 \pm 0.01\%$, whereas that for ip injection was up to $77.4 \pm 28.0\%$.¹¹ Therefore, to develop an amentoflavone formulation with high oral bioavailability is imminent before further investigation on its antidiabetic mechanisms.

In recent years, micelle-based drug delivery systems are widely developed because of their enhanced pharmacokinetics, biodistributions, and high stability.¹² We have reported a

Received: February 21, 2019

Accepted: March 12, 2019

Published: March 12, 2019

micelle-based formulation by which the oral bioavailability of the delivered agent was improved greatly.¹³ Importantly, nano-based systems for antidiabetic application have been paid more attention as they could supply sustained drug release to regulate blood glucose levels (BGLs) for an extended period, decreasing pain caused by frequent injections and certain unwanted gastrointestinal symptoms.^{14–16} Indeed, for antidiabetic drug targeting to multiple tissues, the micelle-based drug delivery system may optimize the biodistribution of the agent.¹⁷ NVP is a highly hydrophilic monomer that possesses desirable properties such as bioadhesion and minimal toxicity.^{18,19} The addition of NVP could enhance the mucoadhesion behavior of nanoparticles on intestinal tissue. On the other hand, the original guerbet alcohols have two chains differing in length by two methylene groups, making it less volatile. Moreover, the two chains with different lengths make it possible to entrap more drug molecules when these chains arranged to form the cores of micelles because of more space.²⁰ Overall, when NVP was grafted by guerbet alcohols, micellar solution could be easily self-assembled because of the enlargement in the hydrated NVP headgroup.²¹ Besides, this self-assembly ability also related to the stronger hydrogen bonding capabilities relying on the interactions between N atoms and carboxyl groups. Therefore, such micelles would be in a strong structure at the acid gastrointestinal microenvironment because of the enhanced hydrogen bond strength, resulting in less drug leakage. In blood, these micelles may become more loose, making it possible to release the loaded drug. Therefore, it urged us to explore whether amentoflavone-loaded micelles could achieve a high bioavailability.

In this study, the aim of this work was to develop an amentoflavone-loaded micelle system with high oral bioavailability for in vivo treatment of diabetes in a KKAY insulin-resistant diabetes mouse model. It was expected that the micelle formulation would optimize the amentoflavone distribution than the free amentoflavone. In vivo biological activities of the amentoflavone-loaded micelle were explored. The results demonstrated that the bioavailability of AF was significantly improved after loading into the micelles, accompanied by improved biological activities. Most importantly, in vivo studies revealed enhanced effect on regulating the expression and activity of downstream signaling factors and proteins by lowering blood lipids, reducing inflammatory responses, and activating the PPAR signaling pathway and PI3K/Akt signaling pathway.

2. MATERIALS AND METHODS

2.1. Materials. Amentoflavone was purchased from Chengdu Pufei De Biotech Co., Ltd. Metformin hydrochloride tablets were purchased from Shanghai Xinyi Pharmaceutical Factory Co., Ltd. *N*-vinyl pyrrolidone-maleate-guerbet alcohol monoester (NVP-MGAM) polymer ($M_w = 22.2$ kDa) was provided by Professor Yurong Hu from Zhengzhou University. Nuclear magnetic resonance spectroscopy, Fourier transform infrared spectroscopy, gel permeation chromatography, and elemental analysis of the synthesized P(NVP-MGAM) results were provided in Figure S1. All other agents belonging to analytical grade were used without further purification.

All the experimental animals were fed special food and cared according to the criteria of the national regulation on the management of laboratory animals.

2.2. Preparation of P(NVP-MGAM)/AF Micelles. P(NVP-MGAM)/AF micelles were prepared by a dialysis method.²² Briefly, AF and NVP-MGAM were codissolved in dimethyl sulfoxide. The solution was loaded into a dialysis tube (cutoff mass 12 000 Da).

Then, this tube was immersed in 1 L ultrapure water for 72 h. The replacement of water was carried out four times every day. After the dialysis process, the solution was centrifuged to remove the excess product. The collected solution was filtered with a filtering membrane (0.22 μm). Besides, thin-film hydration method and emulsion process were used as described previously, respectively.¹³

2.3. Characterization of P(NVP-MGAM)/AF Micelles. The size distribution and zeta potential of micelles were measured by dynamic light-scattering method with a Malvern Zetasizer Nano-ZS90 (Malvern Instruments, Malvern, UK). The atomic force microscopy (AFM) image was captured by using the tapping mode with a setting of 512 pixels/line and 1 Hz scan rate with a Nanoscope IIIa controller (Veeco, Santa Barbara, CA). The morphology of the micelles was observed with a cryogenic transmission electron microscope (Cryo-TEM, FEI Tecnai 20, Netherlands).

The AF encapsulation efficiency referred to the percentage of encapsulated AF with respect to the total amount of AF. Briefly, P(NVP-MGAM)/AF micelles were diluted with methanol and subjected to sonication for 0.5 h. The obtained solution was centrifuged at 12 000 rpm for 5 min. The supernatant was determined by high-performance liquid chromatography (HPLC). The separation was achieved on a C18 column (Agilent Eclipse XDB-C18, 4.6 mm \times 250 mm, 5 μm) at a flow rate of 1.0 mL/min. The mobile phase was composed of methanol (A) and 0.1% phosphoric acid (B) and the following gradient solvent system was adopted: 0–30 min, A/B = 3/2; 30–45 min, 60–85% A, 40–15% B. The detection wavelength was set at 330 nm and the column temperature was kept at 30 $^{\circ}\text{C}$.

The stability of the P(NVP-MGAM)/AF micelles was carried out in a simulated gastric fluid (SGF) and simulated intestinal fluid (SIF), respectively. Briefly, the size distribution of the P(NVP-MGAM)/AF micelles dispersed in the SGF or SIF was monitored by dynamic light-scattering method.

In vitro release behaviors were performed by using a dialysis method. The release media were SGF, SIF, or phosphate-buffered solutions. Briefly, the dialysis bags loaded with P(NVP-MGAM)/AF micelles or AF were first soaked in 50 mL of SGF and were shaken in a horizontal shaker at 100 rpm for 2 h. Thereafter, they were placed in 50 mL of SIF for further shaking. The other group with phosphate-buffered saline (PBS) (pH 7.4) as the control was also carried out simultaneously. At predetermined time points, 2 mL of the samples was taken out and an equal volume of the fresh medium was added.

2.4. In Vivo Pharmacokinetics. Sprague–Dawley (SD) rats were purchased from Henan Experimental Animal Center. The pharmacokinetic properties of free AF and P(NVP-MGAM)/AF micelles were evaluated in SD rats ($n = 3$). Briefly, SD rats were allowed to fast overnight. AF and P(NVP-MGAM)/AF were orally administrated. The dosage of AF was 8.0 mg/kg. Blood samples were collected at different times after injection. The collected plasma was further treated and analyzed by ultra-HPLC–tandem mass spectrometry (Agilent 1290 Infinity, Agilent, USA).

Chromatographic separation was achieved on a ZORBAX RRHD Eclipse C18 (2.1 mm \times 50 mm, 1.8 μm , Agilent Technologies, USA) by gradient elution. The mobile phase was methanol/water (V/V = 60:40) containing 0.1% formic acid with a flow rate of 0.3 mL/min. Luteolin was used as an internal standard material. The detection was completed on a triple quadrupole mass spectrometer (Agilent 6460 Triple Quad, Agilent, USA) with positive electrospray ionization in a multiple reaction-monitoring mode. The pharmacokinetic parameters were computed by using noncompartment assessment with the PK solver software (China Pharmaceutical University, Nanjing, China).

Besides, the SD rats were allowed to fast overnight and administrated two formulations as described above. After administration for 0.5, 2, 6, and 8 h, each SD rat in the two groups was euthanized. The major organs, including heart, liver, spleen, lungs, kidneys, stomach, and small intestine, were collected, weighed, and homogenized in saline. The samples were further treated and measured as described above.

2.5. Biological Effect Study. KKAY mice were obtained from Beijing Hfk Bioscience Co, Ltd. All the mice received care in compliance with the criteria of the national regulation on the

Table 1. Physicochemical Characteristics of Micelles

polymer weight (mg)	drug weight (mg)	size distribution (nm)	PDI	zeta potential (mV)	encapsulation efficiency (%)	loading efficiency (%)
80	20	66.28 ± 4.39	0.34	−2.21 ± 0.05	68.72 ± 2.27	6.01 ± 0.80
100	20	58.8 ± 1.29	0.17	−5.26 ± 0.63	84.39 ± 2.28	14.06 ± 0.10
120	20	54.18 ± 3.19	0.53	−1.28 ± 0.88	82.11 ± 3.42	10.25 ± 0.40

management of laboratory animals. All animal experiments were performed in compliance with the protocol approved by the ethics committee of Zhengzhou University. KKAy mice were fed chow consisting of 37.89% carbohydrates, 14.46% protein, 45.65% fat, 1.00% fiber, minerals, and vitamins (Hfk Bioscience Co., Ltd., China). Sixty KKAy mice with a higher glucose level (>13.9 mmol/L) were randomly divided into four groups: (1) control group, (2) oral metformin (0.01 mL/g, 0.2 g/kg), (3) oral P(NVP-MGAM)/AF micelles (0.01 mL/g, 0.2 g/kg), and (4) oral AF (0.01 mL/g, 0.2 g/kg). Each mouse was administrated one time per day for 6 weeks. Ten C57 BL/6J mice (8 weeks) were assigned to the normal group. During the therapeutic period, water consumption, food intake, and body weight were monitored. Besides, parallel experimental groups for regular insulin (RI) administration via ip were set in order to evaluate whether the treatments could help insulin to activate the PI3K-Akt pathway. The RI was administrated at a dose of 5 mU/g.

2.5.1. Analysis of Metabolic Parameters. During the experimental period, blood samples were collected from these mice at predetermined times and further determined with a Celercare M Automatic biochemical analyzer (Tianjin MNC Technologies Co., Ltd., China). Other biochemical analysis items included triglycerides (TG), low-density lipoprotein cholesterol (LDL-C), high-density lipoprotein cholesterol (HDL-C), cholesterol (CHOL), and glycosylated serum protein (GSP). Besides, free-fatty acids (FFA), a hypersensitive C-reactive protein (hs-CRP) and tumor necrosis factor alpha (TNF- α) were determined with the corresponding kits from R&D systems. At the end of 6 weeks of treatment, the mice were allowed to fast for 10 h and the blood samples were collected, and plasma was obtained by centrifugation at 3000g for 10 min. The plasma insulin levels and glycosylated hemoglobin (GHb) were detected with the Mouse Insulin ELISA Kit and Mouse GHb ELISA KIT (Nanjing Jiancheng Bioengineering Institute), respectively.

The quantitative insulin sensitivity check index (QUICKI) was calculated with a reported formula:²³ (QUICKI = $1/\{\log[\text{fasting insulin } (\mu\text{IU/mL}) + \text{fasting glucose } (\text{mg/dL})]\}$).

2.5.2. Oral Glucose Tolerance Test. Oral glucose tolerance test (OGTT) was performed to detect the long-term in vivo glucose responsiveness of different treatments at the end of 5 weeks of treatments. Briefly, mice were administrated with different formulations for 5 weeks. The initial BGL was determined, and a glucose solution was then injected ig 2 g/kg. The BGL was determined with an Accu-Chk active blood glucose meter (Roche, Germany) at 30, 60, and 120 min after administration. The area under the curve (AUC) of blood glucose versus time was analyzed by using the following formula:

$$\begin{aligned} \text{AUC}(\text{mmol/L}\cdot\text{h}) = &[(\text{BGL0} + \text{BGL30}) \times 0.25] \\ &+ [(\text{BGL30} + \text{BGL60}) \times 0.25] \\ &+ [(\text{BGL60} + \text{BGL120}) \times 0.5] \end{aligned}$$

2.5.3. Histological Analysis and Tissue Microarray Assay. The tissue microarray assay (TMA) blocks (2 mm × 2 mm in dimension) of liver or pancreas were prepared and their sections were used for hematoxylin–eosin (H&E) assessment and immunohistochemical stains, respectively. Meanwhile, mouse liver and skeletal muscle tissues were collected, and glycogen levels or muscle glycogen were measured by colorimetric assay according to the protocol (Jiancheng Biotechnology, Nanjing, China).

Immunohistochemistry was performed following the routine protocol. Rabbit anti-PPAR gamma antibody (bs-0530R), rabbit anti-GLUT2 antibody (bs-0351R), rabbit anti-phospho-AKT1 (Ser473) antibody (bs-12456R), and rabbit anti-IRS1 antibody (bs-

0172R) were purchased from Beijing Biosynthesis Biotechnology Co., Ltd., Beijing, China. After immunostaining, these TMA slides were scanned with Scanscope CS (Aperio Technologies, United Kingdom).

2.5.4. Western Blotting Test. Liver or skeletal muscle lysates were subjected to lysis with a radioimmunoprecipitation assay buffer, including protease and phosphatase inhibitors. The total protein concentrations were determined by using the BCA protein assay kit (Beyotime Biotechnology, China). The cell lysates were subjected to sodium dodecyl sulfate–polyacrylamide gel electrophoresis and electrotransferred from the gel onto a polyvinylidene difluoride membrane followed by incubation with the primary antibodies anti-IR-1, anti-PI3K, anti-p-Akt-ser473, and foxo1 (Beijing Biosynthesis Biotechnology Co., Ltd.). The proteins were monitored with an enhanced chemiluminescence method.

2.5.5. Quantitative Real-Time PCR Analysis. Total RNAs were extracted from fresh frozen mouse liver tissues or skeletal muscle tissues by using the TRIzol reagent (Shanghai Sangon Biotech Co., Ltd.), according to the manufacturer's protocol.

For quantitative polymerase chain reactions (PCRs), cDNA was synthesized with oligo(dT) 18 primer and the reverse transcription kit (Shanghai Sangon Biotech Co., Ltd.). Quantitative PCRs (qPCRs) with a final volume of 20 μL containing primer solution, SybrGreen qPCR Master Mix (Shanghai Sangon Biotech Co., Ltd.), and cDNA were performed with an ABI Step One Plus real-time PCR system (Life technologies, USA). PCR primers for β -actin, PPAR γ , Glut-2, and Glut-4 were summarized in Table S1. The PCR was carried out according to the manufacturer's protocol. The results were calculated by using the $2^{-\Delta\Delta C_T}$ methods.

2.5.6. Cytotoxicity of the Blank Micelles. 3T3 cells were used for evaluating the cytotoxicity of the blank micelles. First, the cells were plated on a 96-well plate. After overnight incubation, different concentrations of the blank micelles were added to the cells. After incubation for 48 h, the MTT test was performed for evaluating the cytotoxicity of the blank micelles.

3. STATISTICAL ANALYSIS

Data are listed as mean \pm standard deviation. Differences between the groups were assessed by using Student's *t*-test while the analysis of variance was adopted to estimate the statistical significance for more than two groups.

4. RESULTS AND DISCUSSION

4.1. Preparation and Characterization of Micelles.

Considering that efficient loading of AF into the P(NVP-MGAM) micelles is dominant, we utilized different methods to prepare P(NVP-MGAM)/AF micelles. The emulsion method failed to produce micelles because precipitation occurred during the process. In comparison with the dialysis method and solvent evaporation method, the polydispersity index (PDI) of the micelles obtained by the dialysis method is lower than that in the latter method. Therefore, the dialysis method was chosen to prepare AF micelles based on the P(NVP-MGAM) polymer. However, it is worthy of exploration to encapsulate other therapeutic agents with this polymer by using other different methods.^{24,25}

In order to understand the role of the weight ratio of the polymer in the AF micelles, a series of micelles with different polymer ratios was prepared. As shown in Table 1, when the ratio of polymer to drug was 5:1, the AF micelles possessed the

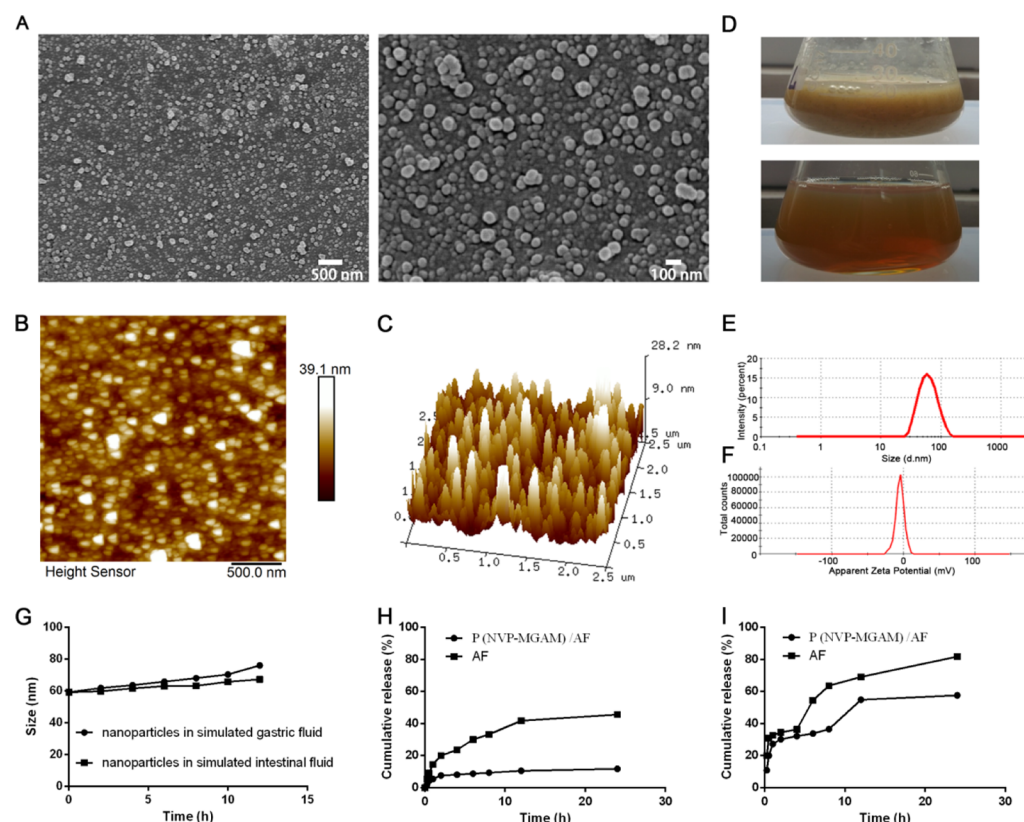


Figure 1. Characterization of P(NVP-MGAM)/AF micelles. (A) TEM image, (B) AFM height image, (C) AFM three-dimensional image, and (D) appearance of AF solution (above) and P(NVP-MGAM)/AF micelles (below). (E) Size distribution and (F) zeta potential. (G) Size change of P(NVP-MGAM)/AF micelles. (H) Leakage of AF, which was carried out for first 2 h in pH 1.2 SGF, the following 22 h in pH 6.5 SIF. (I) Cumulative percentage of released AF in pH 7.4 PBS.

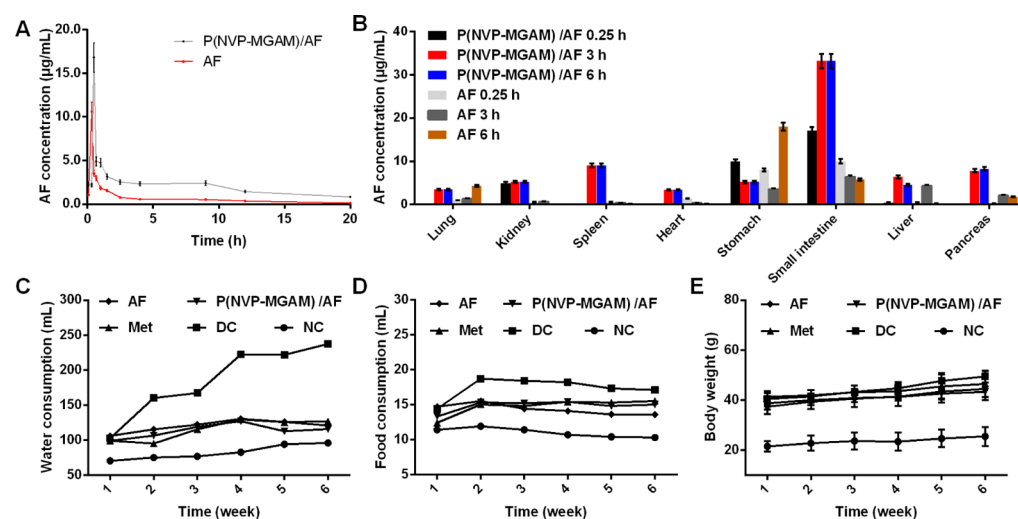


Figure 2. In vivo assessment of AF formulations. (A) Plasma concentration–time curves of AF in rats after oral administration of AF formulations. (B) Tissue distribution of P(NVP-MGAM)/AF and AF at 0.25, 3, and 6 h, respectively. (C) Effects of different treatments in KKAY mice on water consumption during the therapeutic period. (D) Effects of different treatments in KKAY mice on food intake during the therapeutic period. (E) Effects of different treatments in KKAY mice on body weight during the therapeutic period.

higher encapsulation efficiency ($84.39 \pm 2.28\%$) and loading efficiency ($14.06 \pm 0.10\%$). Besides, the AF micelles also possessed a lower PDI and the size distribution was 58.8 ± 1.29 , indicating a good stability.

As shown in Figure 1A–C, the TEM and AFM images showed that these nanoparticles were almost spherical in shape. Figure 1D showed that the native AF suspension

appeared as insoluble residues and precipitation occurred in a short time while the AF micelles looked transparent because of the encapsulation of AF into micelles. The micelles size and zeta potential of P(NVP-MGAM)/AF was 58.44 ± 2.21 nm (Figure 1E) and -4.98 ± 0.59 mV (Figure 1F), respectively.

When oral micelles are prepared as the AF carrier, their stability in the gastrointestinal tract should not be ignored.

Table 2. Pharmacokinetics of P(NVP-MGAM)/AF and AF after Oral Administration

parameters	unit	AF	P(NVP-MGAM)/AF
$t_{1/2}$	h	5.02 ± 0.17	17.89 ± 1.16
T_{max}	h	0.33 ± 0.01	0.67 ± 0.07
C_{max}	$\mu\text{g/mL}$	10.6 ± 0.84	16.83 ± 1.04
AUC_{0-t}	$\mu\text{g}/(\text{mL h})$	16.1 ± 1.86	52.70 ± 2.16
MRT_{0-inf_obs}	h	5.66 ± 1.26	23.45 ± 1.02
V_{z_obs}	$(\text{mg/kg})/(\mu\text{g/mL})$	3.41 ± 2.23	2.30 ± 0.18
Cl_{obs}	$(\text{mg/kg})/(\mu\text{g/mL})/\text{h}$	0.47 ± 0.08	0.09 ± 0.01

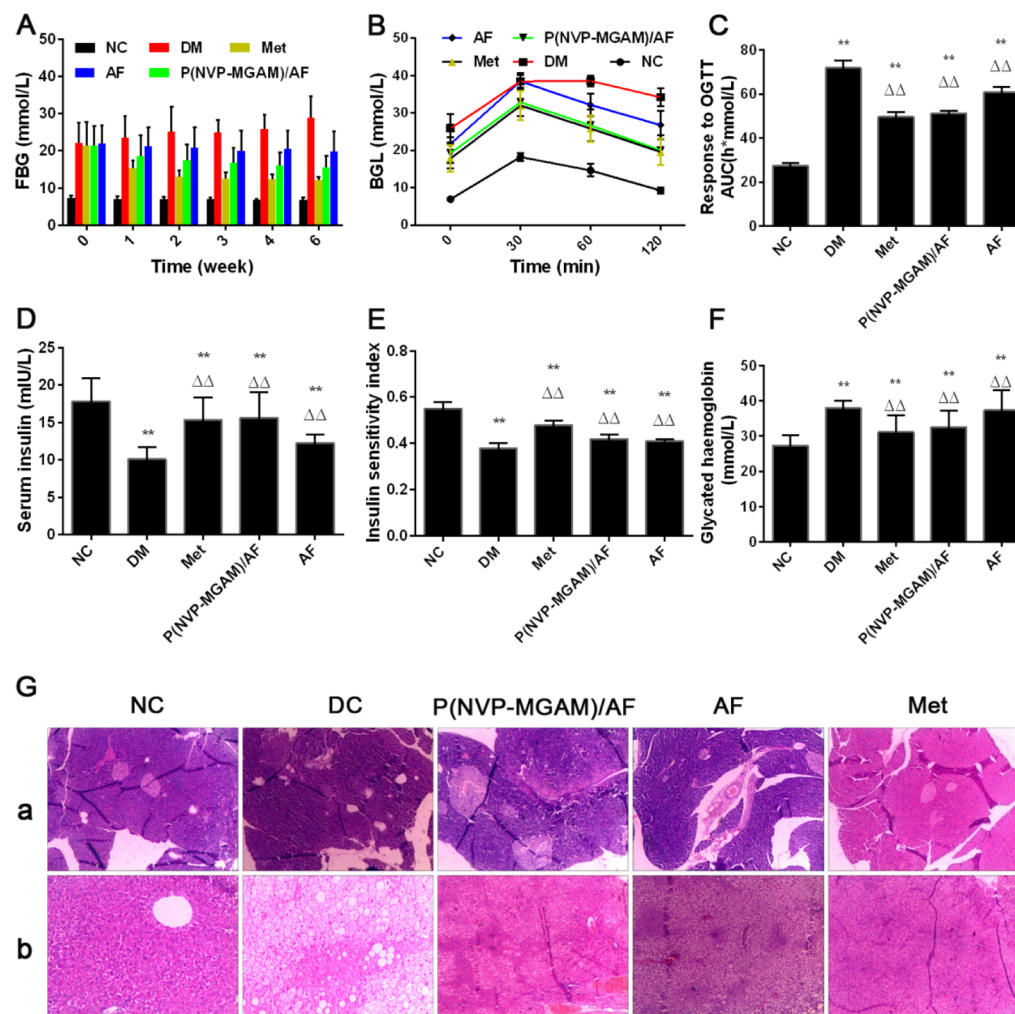


Figure 3. In vivo evaluation of AF formulations in a KKay mice model. (A) Long-term BGL measurement after different treatments in all experimental groups. (B) Intraperitoneal glucose tolerance test result of diabetic mice after 2 h administration of AF, P(NVP-MGAM)/AF compared with C57 BL/6J mice. (C) Calculated responsiveness to OGTT according to the area under the time vs BGL curve over 2 h. (D) Serum insulin level after different treatments. (E) Insulin sensitivity index after different treatments. (F) GHb levels after different treatments. (G) H&E staining of pancreas (a) and liver (b) tissue after different treatments.

Therefore, the stability of P(NVP-MGAM)/AF micelles was measured by understanding the changes of their particle size upon incubating with SGF and SIF, respectively. Interestingly, Figure 1G showed that no obvious change in particle size was detected for P(NVP-MGAM)/AF micelles both in SGF and SIF. This observation indicated that the P(NVP-MGAM) polymer could stand up to the test of the complex gastrointestinal tract and turned out to be a good carrier for AF oral administration.

It is well-known that micelles for oral administration will be subjected to a severe gastrointestinal microenvironment and

should be capable of migrating upstream through the mucus layer that is in rapid renewal.²⁶ Therefore, the AF leakage in SGF and SIF may also be an indicator for oral antidiabetic application. As shown in Figure 1H–I, the cumulative percentage of released AF from P(NVP-MGAM)/AF was lower than that of AF solution. Importantly, the released AF was lower than 20% in 24 h. This profile is beneficial for enhanced oral absorption of AF. Interestingly, the release of AF from P(NVP-MGAM)/AF micelles was about 60% at 24 h in pH 7.4 PBS. These profiles may be due to the structure changes of the micelles based on the P(NVP-MGAM)/AF in

different media. In the SGF with pH 1.2 or SIF with pH 6.5, P(NVP-MGAM)/AF may be more stable, leading to good stability and lower drug release. According to the structure of the micelles, we believe that the hydrogen bonds played important roles in forming the self-assembly micelles. Therefore, it is not surprising that the release is inhibited in the acid medium because of the enhanced hydrogen bonding capabilities. However, in the PBS with a pH 7.4, the disassembly of P(NVP-MGAM)/AF micelles may be accelerated because of the loose structure, resulting in a higher drug release level.

4.2. Pharmacokinetic and Tissue Distribution of P(NVP-MGAM)/AF Micelles and AF Solution. The mean plasma concentration-time curves of P(NVP-MGAM)/AF and AF via oral administration are shown in Figure 2A. The pharmacokinetic parameters, such as $t_{1/2}$ and AUC et al., were summarized in Table 2. Compared with oral native AF suspension, oral P(NVP-MGAM)/AF group not only delayed the T_{max} but also prolonged the retention time of AF in blood by about 4.1 times. The AUC of P(NVP-MGAM)/AF was higher than that of AF suspension with a 2.3-fold increase. The clearance of AF and P(NVP-MGAM)/AF was 0.47 ± 0.08 and 0.09 ± 0.01 (mg/kg)/(μg/mL)/h, respectively, indicating that the micelles were slowly metabolized in the body. The tissue distributions of P(NVP-MGAM)/AF and AF at 0.25, 3, and 6 h are shown in Figure 2B. The distribution of P(NVP-MGAM)/AF in each tissue was significantly higher than that in the AF suspension group, indicating that the bioavailability of P(NVP-MGAM)/AF was improved. With the extension of time, the AF concentration in the small intestine was increased and remained at a high level up to 6 h, suggesting that the micelles formulation is easily absorbed by the small intestine. This enhanced uptake/absorption phenomenon of the drug delivered by the micelles could be attributed to two reasons. On the one hand, NVP is a highly hydrophilic monomer that possesses desirable properties such as bioadhesion, which resulted in improved adhesion on the intestinal wall. On the other hand, the small size (58.44 nm) and viruslike neutral charged surface (−4.98 mV) of the micelles achieved rapid mucus penetration, which also promoted the enhanced absorption intestine in vivo.²⁷ Moreover, this phenomenon was also reported by a prior study. Overall, the concentration of P(NVP-MGAM)/AF micelles also exhibited higher levels in the spleen, liver, and pancreas. This result would be of great benefit for AF efficacy because these organs are easily subjected to the damages caused by diabetes. Besides, it was proved that there is more content in the kidney for native AF suspension, which confirmed that free AF is mainly excreted through the kidney.

Oral nanoformulation was promising as a drug delivery system to treat T2DM because it could conquer the shortcoming of the short half-life of the agent and achieve sustained efficiency.²⁸ Our findings showed that this formulation could act as a promising candidate for future clinical application of AF for type-2 diabetes treatment.

4.3. Biological Effect Study of AF Formulations for T2DM Treatment. **4.3.1. Effects of AF Formulations on Water Consumption, Food Intake, and Body Weight.** KKAY mice were defined as glucose-intolerant black KK mice with the yellow obese gene.²⁹ Obese, hyperinsulinemic, and hyperglycemic characteristics would appear on the KK-Ay mice fed with a regular high-fat diet, which are very similar to the characteristics of T2DM in human. In the present study,

KKAY mice were bred as a T2DM animal model to understand the antidiabetic effects of AF formulations in vivo. During the experiment period, water consumption, food intake, and body weights were monitored. Figure 2C–E shows that water consumption and food intake of KKAY mice in the DM group were significantly higher than that in the NC group, resulting in a significant increase of body weight at the end of the study. However, the AF treatments increase the body weight for the KKAY mice.

4.3.2. Effects of AF Formulations on T2DM Hyperglycemia. Changes of BGL after administration of different formulations are shown in Figure 3A. Metformin, a widely used first-line antidiabetic drug, was chosen as a positive agent. Following 2 weeks of oral medication, all the therapeutic KKAY mice in the Met, AF, and P(NVP-MGAM)/AF groups showed decreased BGLs. In contrast, higher BGL was observed in the DM group. Importantly, the antihyperglycemic activity of AF formulations was comparable to that of Met. Results of a glucose tolerance test in diabetic KKAY mice and C57BL/6 mice performed at the end of 6 weeks of treatments are shown in Figure 3B,C.

Glucose administration in OGTT resulted in an increase of BGLs, which peaked at 30 min. For DM group, the BGL still remained higher at 120 min. Mice administrated with Met and AF formulations revealed a notable improvement in overall glucose response following glucose loading. Considering the lower BGL for mice treated with metformin and P(NVP-MGAM)/AF at 120 min following administration, there is no doubt that the better regulation of BGL by these micelles is easy to see. In summary, the glucose-decreasing effect of P(NVP-MGAM)/AF has much superiority to that of native AF suspension.

As shown in Figure 3D, the serum insulin in the DM group was lower than that of other groups. In comparison with the normal control group, serum insulin levels in the diabetic groups were increased obviously after treatments for 6 weeks. Serum insulin in the metformin and P(NVP-MGAM)/AF groups was increased significantly. Subsequently, insulin sensitivity check indexes were calculated and the results further proved that P(NVP-MGAM)/AF could improve the insulin tolerance (Figure 3E).

Oral antidiabetic drugs should be initiated at a low dose and increased in terms of glycemic response, as estimated according to GHb concentration.²⁸ As shown in Figure 3F, the P(NVP-MGAM)/AF-treated mice showed decreased levels of GHb in comparison with the model group.

4.3.3. Effects of AF Formulations on Mouse Pancreas and Liver Histological Changes. The diminished ability of the pancreas to provide insulin because of β -cell damage and malfunction in T2DM usually aggravated hyperglycemia, leading to the development of severe diabetic complications.³⁰ In order to assay whether AF formulations could protect pancreatic β -cells, histological examinations were carried out first. As shown in Figure 3G, the images indicated that the abnormality induced by diabetes was lessened by AF treatments or metformin. In the diabetic mice group, hepatic steatosis was obvious, and empty lipid vacuoles appeared in the liver tissue. After AF formulation treatments for 6 weeks, the extent of hepatic steatosis was reversed, especially in the P(NVP-MGAM)/AF group.

4.3.4. Effects of AF Formulations on TG, FFA, HDL-C, LDL-C, and GSP Levels in the Serum. The lipid content in blood was detected at the endpoint of the study. The results for

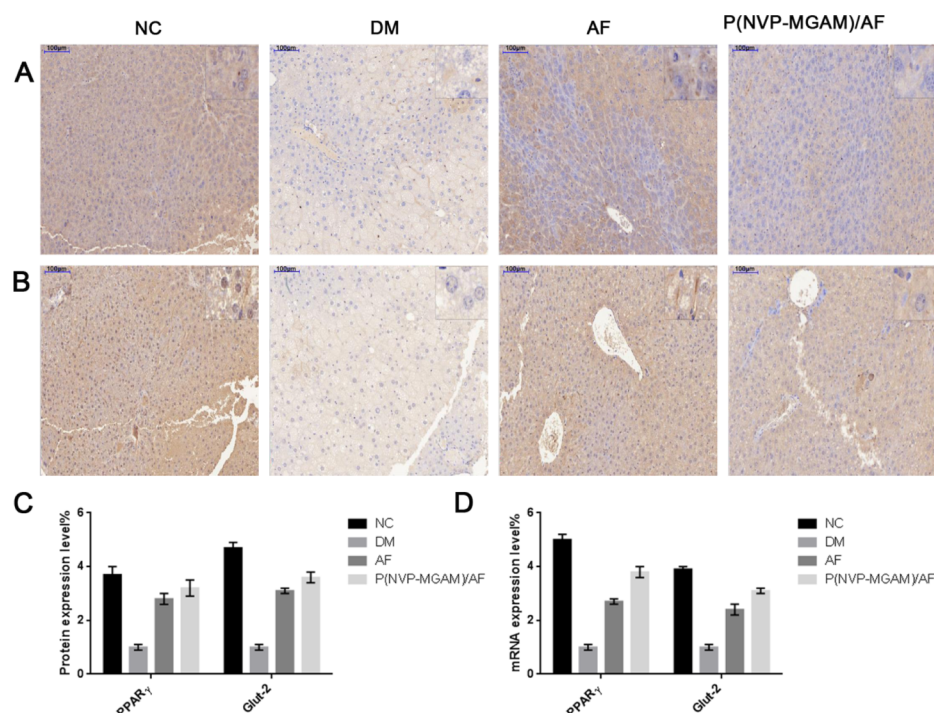


Figure 4. Immunohistochemical staining images of liver tissue microarray and mRNA expression levels. (A) Representative immunohistochemical staining of PPAR γ . (B) Representative immunohistochemical staining of Glut-2. (C) Quantitative results of PPAR γ and Glut-2 protein expression level in liver tissue. (D) Quantitative results of PPAR γ and Glut-2 mRNA expression level in liver tissue. Scale bar: 100 μ m.

serum lipids are shown in Tables S2 and S5. The serum TG, FFA, and LDL-C levels in the AF formulations or metformin-treated groups were obviously lower than those in the DM group ($P < 0.05$), whereas the HDL-C level was higher to some extent. Besides, the GSP levels were also detected, which is shown in Table S6. The result showed that the GSP level could return to normal.

4.3.5. Effects of AF Formulations TNF- α and hs-CRP Levels in the Serum. In general, chronic inflammation in tissues contributed to insulin resistance, which indicated that inflammatory cells secrete proinflammatory cytokines such as TNF- α , resulting in inhibition of insulin signaling pathway.^{31,32} TNF- α has been demonstrated to have certain catabolic influence on fat cells and was believed to be an indicator of T2DM.³³ Besides, elevated hs-CRP is also associated with increased possibility of diabetes.³⁴ As shown in Table S7, compared to the normal group, both TNF- α and hs-CRP levels were elevated significantly ($P < 0.01$). Interestingly, after 6 weeks of treatment, all the therapeutic groups showed decreased TNF- α and hs-CRP levels. In comparison with the native AF suspension, P(NVP-MGAM)/AF has obvious superiority in decreasing the TNF- α and hs-CRP levels. Therefore, AF formulations could be capable of inhibiting secretion of proinflammatory cytokine like TNF- α to reverse insulin resistance.

4.3.6. Effects of AF Formulations on Protein and mRNA Expressions of PPAR γ , Glut-2, and Glut-4 in Diabetic KKAY Mice. Peroxisome proliferator-activated receptor γ (PPAR γ), which is related to lipid homeostasis regulation, could regulate glucose, cholesterol, and cholesterol metabolic disorders.³⁵ Overexpression of PPAR is involved in many metabolic processes, most of which resulted in decreased energy storage. The liver as an insulin-dependent organ played an important role in glucose regulation and lipid metabolism.³⁶ As shown in

Figure 4A, expression levels of PPAR γ were significantly lower in the liver of KKAY mice than in the C57 BL/6J mice, and AF treatments tended to increase this level, suggesting the upregulation of PPAR γ by AF treatment. In comparison, the expression level of PPAR in the P(NVP-MGAM)/AF group is at least equal to better than that of the AF group with higher PPAR level. Also noted was Glu-2 expression levels in this study, which were obviously different on these sections (Figure 4B,C). Its expressions were significantly higher in AF treatments than that of the DM group.

We then compared the relative expression levels of PPAR γ and Glut-2 transcripts in the liver of mice from each group. As shown in Figure 4D, the expression levels of PPAR γ mRNA and Glut-2 mRNA in DM mice were set to 1.0 for all subsequent calculations. In mice from the DC group, PPAR γ and Glut-2 mRNA levels were higher. The relative expression values of them were about 4.7 and 3.9, respectively. In contrast, the therapeutic mice, as expected, exhibited greatly enhanced PPAR γ and Glut-2 transcript levels. Surprisingly, it was the P(NVP-MGAM)/AF formulation which obviously upregulated the transcript levels of two genes, and the increased expression of them is slightly weak for AF suspension.

Glu-2 is a glucose-sensitive transporter, which is also responsible for glucose utilization in liver. Therefore, it is reasonable to suppose that the upregulation of Glut-2 in the liver after AF formulation treatment would result in glycogen deposition in the liver. As shown in Table S8, the AF-treated T2DM group revealed more glycogen storage in the liver. Meanwhile, the muscle glycogen accumulation induced by AF treatments was also detected. In an attempt to study the action of AF treatments on insulin signal transduction in the skeletal muscle tissue, PPAR γ and Glut-4 mRNA levels were also measured by qPCR. As shown in Figure S2, AF treatments significantly enhanced the PPAR γ and Glut-4 mRNA levels in

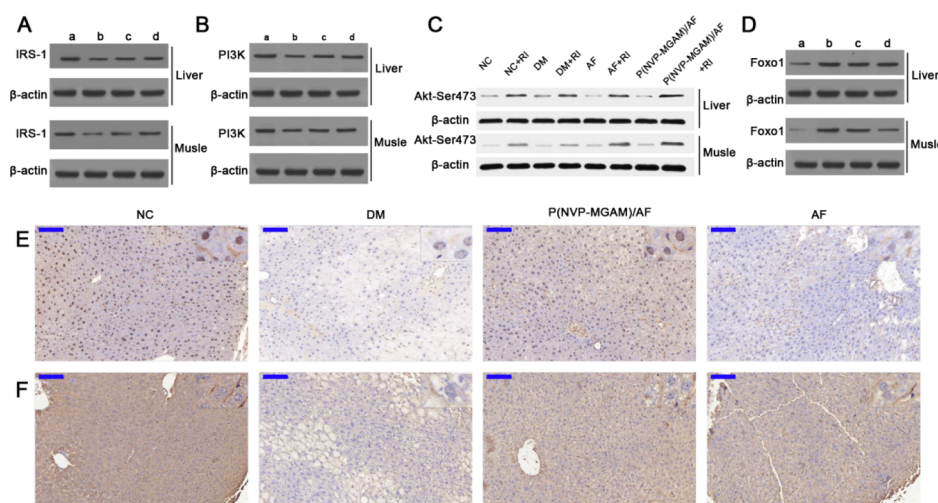


Figure 5. Effect of AF formulations on the protein expression in diabetic KKAY mice compared to the C57 BL/6J mice. (A) Western blot analyses of IRS-1 in liver and skeletal muscle, respectively. (a) NC group; (b) DM group; (c) AF group; and (d) P(NVP-MGAM)/AF group. (B) Western blot analyses of PI3K in liver and skeletal muscle, respectively. (a) NC group; (b) DM group; (c) AF group; and (d) P(NVP-MGAM)/AF group. (C) Western blot analyses of Akt-Ser473 in liver and skeletal muscle, respectively. (D) Western blot analyses of Akt-Foxo1 in liver and skeletal muscle, respectively. (E) Representative immunohistochemical staining of P-Akt. (F) Representative immunohistochemical staining of IRS-1. Scale bar: 100 μ m.

the skeletal muscle of KKAY mice. Moreover, the effect induced by P(NVP-MGAM)/AF was significantly higher than that of AF. These results revealed that AF has an inspiring effect on skeletal muscle insulin transduction and the AF micelle formulation was preferred to AF.

4.3.7. AF Formulations Triggered Insulin Signaling to Increase Insulin Sensitivity. Insulin receptor substrate 1 (IRS-1) and insulin signaling pathway activation played an important role in glucose transport and glucose metabolism in liver and skeletal muscle.^{37,38} The impaired IRS-1 and the devitalization of protein kinase B (AKT) are primary features of insulin resistance in T2DM. In order to explore whether AF was capable of promoting insulin signaling directly, the expression of IRS-1, PI3K, Akt, and Foxo1 in the liver and muscle of mice in four groups were explored, respectively.

As shown in Figure 5A,B, the results showed that the expression levels of IRS-1, PI3K, and Akt of KKAY mice both in liver or muscle were lower than that of the C57 BL/6J mice group, which is consistent with the prior research.³⁹ Interestingly, AF formulations could not only increase the expression of IRS-1, PI3K, and p-AKT both in liver or muscle directly without insulin but also maintain the effect on p-AKT with RI stimulation (Figure 5C). Moreover, P(NVP-MGAM)/AF showed a better effect on insulin signaling pathway compared to AF suspension, indicating that AF micelles improved its effect in vivo. The accumulation of AF micelles in tissues including liver and muscle could explain why PI3K/Akt signal pathway was effectively regulated by AF micelles.

However, it left unknown whether AF treatments could regulate the downstream factors. Foxo1, a kind of the O class of forkhead/winged helix transcription factors (Foxo), was first recognized as an Akt substrate in insulin signaling.^{40,41} Therefore, foxo1 expression levels in four groups were further measured. As shown in Figure 5D, foxo1 in KKAY mice both in liver or muscle showed a higher level as compared to that of the C57 BL/6J mice group. After AF treatments, as expected, the expression level of foxo1 both decreased obviously. Therefore, it is reasonable to conclude that AF significantly increased the levels of PI3K, AKT to activate the PI3K/AKT/

mTOR signaling pathway, and thereby prevented the insulin resistance.

Figure 5E,F shows P-Akt and IRS-1 staining in the liver. The overall staining of the DM sections was generally lighter than that of the NC sections. As expected, the high levels of P-Akt and IRS-1 in liver were also verified in AF formulation-treated mice. These results indicated that AF activated the insulin signaling, resulting in increased glycogen synthesis in the T2DM rats, restored glucose homeostasis in liver, and promoted glucose uptake and glycolysis in skeletal muscle. In vitro experiments were performed to assess the cytotoxicity of the blank micelles. As shown in Figure S3, the results showed that there is no obvious cytotoxicity.

CONCLUSIONS

In conclusion, oral bioavailability of AF was improved significantly with the simple micelle system based on P(NVP-MGAM). The antidiabetic efficacy of AF was comprehensively investigated first, and our findings showed that AF formulation could play a pivotal role for the treatment of type 2 diabetes, and the effect of it is comparable to that of metformin. The comprehensive effect of AF was achieved by regulating the expression and activity of downstream signaling factors and proteins by lowering blood lipids, reducing inflammatory responses, activating the PPAR γ signaling pathway and PI3K/Akt signaling pathway. In summary, our study provided a basis for the application of AF for treating T2DM, and the developed AF micelle system was worthy of further investigation and use.

ASSOCIATED CONTENT

Supporting Information

The Supporting Information is available free of charge on the ACS Publications website at DOI: 10.1021/acsami.9b03275.

Primer pairs of genes, effects of different treatments on blood biochemical indicators in the serum, characterization of NVP-MGAM, quantitative results of PPAR γ

and Glut-4 mRNA expression level in the skeletal muscle tissue, and cytotoxicity of the blank micelles (PDF)

AUTHOR INFORMATION

Corresponding Author

*E-mail: zhangzz08@126.com. Phone: 86-371-67781910. Fax: 86-371-67781908.

ORCID

Zhenzhong Zhang: 0000-0001-7564-0860

Notes

The authors declare no competing financial interest.

ACKNOWLEDGMENTS

This study was supported by the National Natural Science Foundation of China (nos. 81573364 and 81874304) and the scientific and technological project of Henan Province (no. 162102310067).

REFERENCES

- (1) Hannon, T. S.; Arslanian, S. A. The Changing Face of Diabetes in Youth: Lessons Learned From Studies of Type 2 Diabetes. *Ann. N. Y. Acad. Sci.* **2015**, *1353*, 113–137.
- (2) Rathmann, W.; Giani, G. Global Prevalence of Diabetes: Estimates for the Year 2000 and Projections for 2030. *Diabetes Care* **2004**, *27*, 2568–2569.
- (3) Kim, K.; Kim, E. S.; Rhee, S. Y.; Chon, S.; Woo, J.-t.; Yu, S.-Y. Clinical Characteristics and Risk Factors for Retinal Diabetic Neurodegeneration in Type 2 Diabetes. *Acta Diabetol.* **2017**, *54*, 993–999.
- (4) Fang, P.; Shi, M.; Zhu, Y.; Bo, P.; Zhang, Z. Type 2 Diabetes Mellitus as a Disorder of Galanin Resistance. *Exp. Gerontol.* **2016**, *73*, 72–77.
- (5) Kim, J.-S.; Kwon, C.-S.; Son, K. H. Inhibition of Alpha-Glucosidase and Amylase by Luteolin, a Flavonoid. *Biosci., Biotechnol., Biochem.* **2000**, *64*, 2458–2461.
- (6) Yang, X.; Yang, J.; Xu, C.; Huang, M.; Zhou, Q.; Lv, J.; Ma, X.; Ke, C.; Ye, Y.; Shu, G.; Zhao, P. Antidiabetic Effects of Flavonoids From *Sophora Flavescens* EtOAc Extract in Type 2 Diabetic KK-ay Mice. *J. Ethnopharmacol.* **2015**, *171*, 161–170.
- (7) Kuai, M.; Li, Y.; Sun, X.; Ma, Z.; Lin, C.; Jing, Y.; Lu, Y.; Chen, Q.; Wu, X.; Kong, X.; Bian, H. A Novel Formula Sang-Tong-Jian Improves Glycometabolism and Ameliorates Insulin Resistance by Activating PI3K/AKT Pathway in Type 2 Diabetic KK-ay Mice. *Biomed. Pharmacother.* **2016**, *84*, 1585–1594.
- (8) Kim, H. K.; Son, K. H.; Chang, H. W.; Kang, S. S.; Kim, H. P. Amentoflavone, a Plant Biflavone: A New Potential Anti-Inflammatory Agent. *Arch. Pharmacol. Res.* **1998**, *21*, 406–410.
- (9) Beidokhti, M. N.; Lobbens, E. S.; Rasoavaivo, P.; Staerk, D.; Jäger, A. K. Investigation of Medicinal Plants From Madagascar Against DPP-IV Linked to Type 2 Diabetes. *S. Afr. J. Bot.* **2018**, *115*, 113–119.
- (10) Kim, J.-S.; Kwon, C.-S.; Son, K. H. Inhibition of Alpha-Glucosidase and Amylase by Luteolin, a Flavonoid. *Biosci., Biotechnol., Biochem.* **2000**, *64*, 2458–2461.
- (11) Liao, S.; Ren, Q.; Yang, C.; Zhang, T.; Li, J.; Wang, X.; Qu, X.; Zhang, X.; Zhou, Z.; Zhang, Z.; Wang, S. Liquid Chromatography-Tandem Mass Spectrometry Determination and Pharmacokinetic Analysis of Amentoflavone and its Conjugated Metabolites in Rats. *J. Agric. Food Chem.* **2015**, *63*, 1957–1966.
- (12) Kesharwani, P.; Gorain, B.; Low, S. Y.; Tan, S. A.; Ling, E. C. S.; Lim, Y. K.; Chin, C. M.; Lee, P. Y.; Lee, C. M.; Ooi, C. H.; Choudhury, H.; Pandey, M. Nanotechnology Based Approaches for Anti-Diabetic Drugs Delivery. *Diabetes Res. Clin. Pract.* **2018**, *136*, 52–77.
- (13) Guo, X.; Chen, C.; Liu, X.; Hou, P.; Guo, X.; Ding, F.; Wang, Z.; Hu, Y.; Li, Z.; Zhang, Z. High Oral Bioavailability of 2-Methoxyestradiol in PEG-PLGA Micelles-Microspheres for Cancer Therapy. *Eur. J. Pharm. Biopharm.* **2017**, *117*, 116–122.
- (14) Veisheh, O.; Tang, B. C.; Whitehead, K. A.; Anderson, D. G.; Langer, R. Managing Diabetes with Nanomedicine: Challenges and Opportunities. *Nat. Rev. Drug Discovery* **2015**, *14*, 45–57.
- (15) Xu, H.; Yang, P.; Ma, H.; Yin, W.; Wu, X.; Wang, H.; Xu, D.; Zhang, X. Amphiphilic Block Copolymers-Based Mixed Micelles for Noninvasive Drug Delivery. *Drug Delivery* **2016**, *23*, 3063–3071.
- (16) Payyappilly, S.; Dhara, S.; Chattopadhyay, S. Thermoresponsive Biodegradable PEG-PCL-PEG Based Injectable Hydrogel for Pulsatile Insulin Delivery. *J. Biomed. Mater. Res., Part A* **2014**, *102*, 1500–1509.
- (17) Wang, T.; Wang, N.; Song, H.; Xi, X.; Wang, J.; Hao, A.; Li, T. Preparation of an Anhydrous Reverse Micelle Delivery System to Enhance Oral Bioavailability and Anti-Diabetic Efficacy of Berberine. *Eur. J. Pharm. Sci.* **2011**, *44*, 127–135.
- (18) Sajeesh, S.; Sharma, C. P. Mucoadhesive Hydrogel Micro-particles Based On Poly (Methacrylic Acid-Vinyl Pyrrolidone)-Chitosan for Oral Drug Delivery. *Drug Delivery* **2011**, *18*, 227–235.
- (19) Saillenfait, A. M.; Marquet, F.; Sabaté, J. P.; Ndiaye, D.; Lambert-Xolin, A. M. 4-Week Repeated Dose Oral Toxicity Study of N-ethyl-2-pyrrolidone in Sprague Dawley Rats. *Regul. Toxicol. Pharmacol.* **2016**, *81*, 275–283.
- (20) Hashim, R.; Sugimura, A.; Minamikawa, H.; Heidelberg, T. Nature-Like Synthetic Alkyl Branched-Chain Glycolipids: A Review On Chemical Structure and Self-Assembly Properties. *Liq. Cryst.* **2012**, *39*, 1–17.
- (21) Saari, N. A. N.; Mislán, A. A.; Hashim, R.; Zahid, N. I. Self-Assembly, Thermotropic, and Lyotropic Phase Behavior of Guerbet Branched-Chain Maltosides. *Langmuir* **2018**, *34*, 8962–8974.
- (22) Bian, F.; Jia, L.; Yu, W.; Liu, M. Self-Assembled Micelles of N-phthaloylchitosan-g-polyvinylpyrrolidone for Drug Delivery. *Carbohydr. Polym.* **2009**, *76*, 454–459.
- (23) Katz, A.; Nambi, S. S.; Mather, K.; Baron, A. D.; Follmann, D. A.; Sullivan, G.; Quon, M. J. Quantitative Insulin Sensitivity Check Index: A Simple, Accurate Method for Assessing Insulin Sensitivity in Humans. *J. Clin. Endocrinol. Metab.* **2000**, *85*, 2402–2410.
- (24) Payyappilly, S. S.; Panja, S.; Mandal, P.; Dhara, S.; Chattopadhyay, S. Organic Solvent-Free Low Temperature Method of Preparation for Self Assembled Amphiphilic Poly(-Caprolactone)-Poly(Ethylene Glycol) Block Copolymer Based Nanocarriers for Protein Delivery. *Colloids Surf., B* **2015**, *135*, 510–517.
- (25) Payyappilly, S. S.; Dhara, S.; Chattopadhyay, S. The Heat-Chill Method for Preparation of Self-Assembled Amphiphilic Poly(Epsilon-Caprolactone)-Poly(Ethylene Glycol) Block Copolymer Based Micellar Nanoparticles for Drug Delivery. *Soft Matter* **2014**, *10*, 2150–2159.
- (26) Liu, M.; Zhang, J.; Zhu, X.; Shan, W.; Li, L.; Zhong, J.; Zhang, Z.; Huang, Y. Efficient Mucus Permeation and Tight Junction Opening by Dissociable “Mucus-Inert” Agent Coated Trimethyl Chitosan Nanoparticles for Oral Insulin Delivery. *J. Controlled Release* **2016**, *222*, 67–77.
- (27) Wu, J.; Zheng, Y.; Liu, M.; Shan, W.; Zhang, Z.; Huang, Y. Biomimetic Viruslike and Charge Reversible Nanoparticles to Sequentially Overcome Mucus and Epithelial Barriers for Oral Insulin Delivery. *ACS Appl. Mater. Interfaces* **2018**, *10*, 9916–9928.
- (28) Krentz, A. J.; Bailey, C. J. Oral Antidiabetic Agents. *Drugs* **2005**, *65*, 385–411.
- (29) Okazaki, M.; Saito, Y.; Uda, Y.; Maruyama, M.; Murakami, H.; Ota, S.; Kikuchi, T.; Oguchi, K. Diabetic Nephropathy in KK and KK-ay Mice. *Exp. Anim.* **2002**, *51*, 191–196.
- (30) Munder, A.; Israel, L. L.; Kahremany, S.; Ben-Shabat-Binyamini, R.; Zhang, C.; Kolitz-Domb, M.; Viskind, O.; Levine, A.; Senderowitz, H.; Chessler, S.; Lellouche, J.-P.; Gruzman, A. Mimicking Neuroligin-2 Functions in beta-Cells by Functionalized Nanoparticles as a Novel Approach for Antidiabetic Therapy. *ACS Appl. Mater. Interfaces* **2017**, *9*, 1189–1206.
- (31) De Taeye, B. M.; Novitskaya, T.; McGuinness, O. P.; Gleaves, L.; Medda, M.; Covington, J. W.; Vaughan, D. E. Macrophage TNF- α Contributes to Insulin Resistance and Hepatic Steatosis in Diet-

Induced Obesity. *Am. J. Physiol. Endocrinol. Metab.* **2007**, 293, E713–E725.

(32) Ying, W.; Riopel, M.; Bandyopadhyay, G.; Dong, Y.; Birmingham, A.; Seo, J. B.; Ofrecio, J. M.; Wollam, J.; Hernandez-Carretero, A.; Fu, W.; Li, P.; Olefsky, J. M. Adipose Tissue Macrophage-Derived Exosomal miRNAs Can Modulate in Vivo and in Vitro Insulin Sensitivity. *Cell* **2017**, 171, 372–384.

(33) Hotamisligil, G.; Shargill, N.; Spiegelman, B. Adipose Expression of Tumor Necrosis factor- α -Direct Role in Obesity-Linked Insulin Resistance. *Science* **1993**, 259, 87–91.

(34) Parrinello, C. M.; Lutsey, P. L.; Ballantyne, C. M.; Folsom, A. R.; Pankow, J. S.; Selvin, E. Six-Year Change in High-Sensitivity C-reactive Protein and Risk of Diabetes, Cardiovascular Disease, and Mortality. *Am. Heart J.* **2015**, 170, 380–389.

(35) Hamm, J. K.; El Jack, A. K.; Pilch, P. F.; Farmer, S. R. Role of PPAR Gamma in Regulating Adipocyte Differentiation and Insulin-Responsive Glucose Uptake. *Ann. N. Y. Acad. Sci.* **1999**, 892, 134–145.

(36) Bechmann, L. P.; Hannivoort, R. A.; Gerken, G.; Hotamisligil, G. S.; Trauner, M.; Canbay, A. The Interaction of Hepatic Lipid and Glucose Metabolism in Liver Diseases. *J. Hepatol.* **2012**, 56, 952–964.

(37) Hotamisligil, G. k. S.; Peraldi, P.; Budavari, A.; Ellis, R.; White, M. F.; Spiegelman, B. M. IRS-1-mediated Inhibition of Insulin Receptor Tyrosine Kinase Activity in TNF- α - and Obesity-Induced Insulin Resistance. *Science* **1996**, 271, 665–670.

(38) Engelman, J. A.; Luo, J.; Cantley, L. C. The Evolution of Phosphatidylinositol 3-Kinases as Regulators of Growth and Metabolism. *Nat. Rev. Genet.* **2006**, 7, 606–619.

(39) Wang, L.-Y.; Wang, Y.; Xu, D.-S.; Ruan, K.-F.; Feng, Y.; Wang, S. MDG-1, a Polysaccharide From *Ophiopogon Japonicus* Exerts Hypoglycemic Effects through the PI3K/Akt Pathway in a Diabetic KKAY Mouse Model. *J. Ethnopharmacol.* **2012**, 143, 347–354.

(40) Guo, S. Decoding insulin resistance and metabolic syndrome for promising therapeutic intervention. *J. Endocrinol.* **2014**, 220, E1–E3.

(41) Guo, S.; Dunn, S. L.; White, M. F. The Reciprocal Stability of FOXO1 and IRS2 Creates a Regulatory Circuit that Controls Insulin Signaling. *Mol. Endocrinol.* **2006**, 20, 3389–3399.